2012

TU Delft - 19/06/2012

Lodewijk de Vet
4010515

Mentor: Dr.Ir. A. Blom
Second corrector: Dr.Ir. M. Zijlema

TU Delft Delft University of Technology

[THE BEDLOAD LAYER IN A 1D SAND-GRAVEL MORPHODYNAMIC MODEL]

BACHELOR THESIS

Preface

In order to complete their Bachelor, students of the TU Delft write a bachelor thesis. The thesis is a demonstration of the fact that the student is able to apply and combine the acquired knowledge of the Bachelor degree in an autonomous manner.

This thesis is the result of an eight week study and is supported by the section Environmental Fluid Mechanics of Civil Engineering of the TU Delft.

It is important to mention that the bachelor thesis of Jelle van der Zwaag considers the same subject. Both studies are individually developed and are associated for more profundity.

I would like to thank my supervisor Astrid Blom for her good help and her fair critical questions.

Delft, June 2012
Lodewijk de Vet

Contents

Summary

The effective thickness of the bedload layer over a river bed can be schematised as the total volume of bedload sediment that is in transport, divided by the surface. In practice, this layer is considered to have a constant thickness over time. Main question of this thesis is whether this assumption is valid.

By analyzing the mass balance, it is possible to gain an approximation of the reality. By means of numerical approximations, it is possible to build a morphological model which imitates these equations. This imitation makes it possible to analyze the effect of specific parameters on the sediment transport and the bed surface elevation. In this way, the effect of neglecting the derivative over time of the effective thickness of the bedload layer can be investigated.

The model of a river section of the Rhine between Emmerich am Rhein and Lobith results in a maximum influence of the derivative of the effective thickness of the bedload layer on the morphodynamic changes as the result of one flood event that is smaller than 4%.

A parameter study makes it possible to test the obtained result on sensitivity. Because the morphodynamic model is based on a lot of input parameters, a well founded choice between the large variety of parameters has to be made. A rough sensitivity test shows that the at maximum 4% influence on the derivative is subject to a possible variation of approximately a factor 2, depending on the variation in the input parameters.

List of figures

List of tables

1 Introduction

1.1 Problem description

Morphodynamics is the change in the bed surface elevation (i.e. aggradation and degradation of the river bed) due to gradients in the sediment transport rate. Sediment transport can be separated into two components: bedload transport (the sediment which is interacting with the river bed) and suspended load transport (the rest of the sediment which is in transport). In this thesis, the focus will be on the bedload part of the transported sediment.

In order to schematise the time evolution of the mean bed elevation and the composition of the river bed, it is useful to introduce a layer model. Figure 1 shows the schematisation of the river bed consisting of two layers: the active layer which is the part of the bed that can be entrained into transport (represented by δ) and the substrate, which is the sediment below this active layer that is retained from transport by the active layer (it has no contact with the water flow). Both layers might contain the same material (not necessary uniform sediment).

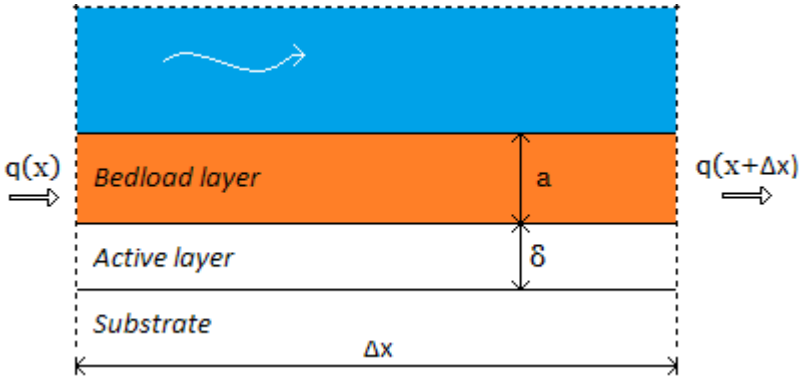

Figure 1 - Schematisation bedload transport

The bedload transport layer is located directly on top of the active layer. Its thickness is schematised with the symbol a. The meaning of this symbol is the total volume of the bedload sediment transport (excluding the pores) divided by its surface in the horizontal plane, therefore:

$$a = \frac{V}{A} \tag{1}$$

So, the bedload layer thickness a is the effective thickness of the bedload sediment when all the sediment would be compounded. In practice, the derivative of a over time is neglected and the question remains if this assumption is allowed. This derivative over time might be important to solve as it is part of the mass conservation equations (see Appendix B.1 and B.2) and is therefore influencing the morphodynamic processes. It requires research in order to estimate how significant this influence is.

It must be clear that neglecting the derivative leads to an easier system to solve (less costs to calculate), but it might result in deviations. In contrast, not neglecting this term results in a more complex system and above all, more data is needed to perform calculations.

1.2 Research questions

The main objective of this bachelor thesis is to produce a model in order to investigate if and under what conditions the effective thickness of the bedload layer is constant over time.

The focus of this thesis will be on the following research questions:

Main research question:

- Under what conditions may the effective thickness of the bedload transport layer in rivers be assumed to be constant in time?

Sub research questions handled in this rapport:

- How do we set up a simple and efficient numerical model for 1D morphodynamics of sand-gravel rivers?
- What is the influence of the time derivative of the effective thickness of the bedload layer on the morphodynamic changes produced by a flood event in the Rhine?
- What is the sensitivity to the parameters in the morphodynamic equations?

1.3 Research methodology

The research questions indicate that this thesis is focused on the construction of a morphodynamic model. The models presented in this thesis are supposed to be the best suitable. Argumentation about the suitability and the choice of input parameters is mainly discussed in the thesis of Jelle van der Zwaag, especially with the focus on flood events in the Rhine.

This thesis is based on the schematisation of the whole sediment distribution as a mixture of two fractions: sand and gravel. The advantage over a uniform schematisation (which contains only one fraction) is a more realistic description of reality (the real distribution is continuously, the more different fractions in the schematisation, the better the approximation). Mention that the uniform schematisation is in fact a special case of the sand-gravel approach (set one of the fraction sizes to one and define one representative sediment size for the whole mixture). A schematisation containing more than two fractions is possible, but it would result in a system of equations which is too complicated for the purpose of this thesis.

The setup of the morphodynamic sand-gravel model starts with the equations related to morphodynamics in Chapter 2. Chapter 3 describes the necessary numerical discretizations and Chapter 4 presents the method of modeling. The model is applied to a reach of the river Rhine in Chapter 5 and the obtained results are analysed. Chapter 6 performs a parameter study in order to check the sensitivity of the influence of the time derivative in effective thickness of the sediment transport layer.

2 Equations related to morphodynamics

This chapter treats the equations relevant for morphodynamic calculations. Division is made between the mass continuity equations and the empirical equations.

2.1 Mass continuity equations

With the establishment of the continuity equations is it possible to treat both sand and gravel fractions as one mixture or to treat both fractions as separate fractions. Please note that both schematisations are valid.

2.1.1 Overall equation of conservation of sediment

Appendix B.1 presents the derivation of the overall equation of conservation of sediment mass, which leads to the conservation equation:

$$c_b \frac{\partial \eta}{\partial t} + \frac{\partial a}{\partial t} = -\frac{\partial q}{\partial x} \tag{2}$$

In this conservation equation, c_b is the sediment concentration within the bed (c_b = 1 – porosity), η the bed surface elevation and, q the specific sediment discharge.

As mentioned in the introduction, the thickness of the bedload layer, a, is equal to the volume of bedload sediment divided by its surface in the horizontal plane. Another expression of this bedload layer thickness is the specific sediment discharge divided by the propagation velocity of the bedload sediment. The total thickness of the bedload layer is therefore defined as:

$$a = a_s + a_g = \frac{q_s}{u_s} + \frac{q_g}{u_g} \tag{3}$$

The calculation of the specific sediment discharge and the propagation velocity of the bedload sediment requires empirical formulations, presented in Chapter 2.2.

2.1.2 Balance equation for the gravel fraction of a sand-gravel sediment mixture

Because the sum of both fractions, by definition, is equal to one, just one fraction has to be calculated, the other fraction follows directly out of the connection:

$$F_g + F_s = 1 \tag{4}$$

In Appendix B.2, the balance equation for the gravel fraction of a sand-gravel sediment mixture is derived, as a variation to the Hirano (1971) active layer model (Figure 2):

$$c_b \delta \frac{\partial F_{mg}}{\partial t} + c_b F_{mg} \frac{\partial \delta}{\partial t} - F_{\mathrm{lg}} \left(\frac{\partial q}{\partial x} + \frac{\partial a}{\partial t} \right) - c_b F_{\mathrm{lg}} \frac{\partial \delta}{\partial t} + \frac{\partial a_g}{\partial t} = -\frac{\partial q_g}{\partial x} \tag{5}$$

In this equation F_{mg} denotes the volume fraction of gravel in the active layer, F_{lg} the volume fraction of gravel at the interface between the active layer and the substrate, c_b the sediment concentration within the bed (= 1 – porosity), δ the thickness of the active layer. The thickness of the active layer, δ, is assumed equal to the bedform height, Δ, which is assumed equal to one fourth of the flow depth:

$$\delta = \Delta = \tfrac{1}{4} H \tag{6}$$

The volume fraction of the gravel in the interface layer between the active layer and the substrate F_{Ig} depends on whether it is a case of aggradation or degradation:

$$F_{Ig} = \begin{cases} F_{mg} & \text{if} \quad \dfrac{\partial \eta_I}{\partial t} > 0 \\ F_{0g} & \text{if} \quad \dfrac{\partial \eta_I}{\partial t} < 0 \end{cases} \qquad (7)$$

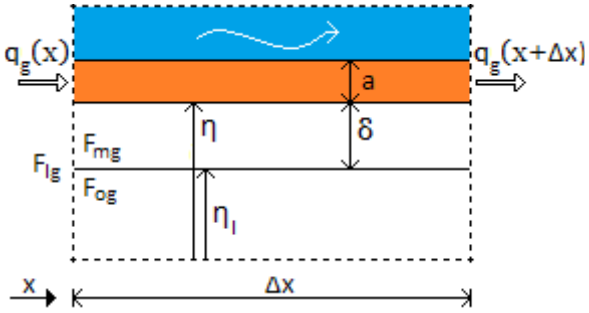

Figure 2 - Hirano active layer model

Mention that the gravel fraction in the active layer, F_{mg}, varies over time according to the balance equation of Equation (5). The gravel fraction in the substrate F_{0g} can vary through a rise of the elevation of the interface layer. A part of the active layer (with composition F_{mg}) will then become part of the substrate. The final substrate does not have to contain a constant gravel fraction over the depth.

2.2 Empirical equations

Sediment transport is a very complicated process. There are no models which imitate the real acting transport on an exact manner. However, empirical formulations give up to a certain extent, a good approximation of the quantity of sediment transported. The choice between the different available empirical formulations is made by Jelle van der Zwaag (accompanying thesis). In fact, we need two quantities related to sediment transport: the volume of bedload transport per unit width and time *q* and the average propagation velocity of the bedload sediment *u*.

The flow depth calculation is also treat as an empirical equation, however it is in fact only partially empirically established.

2.2.1 Volume of bedload transport per unit width and time

Because the gravel fraction has a larger grain size than the sand fraction, the volume of bedload transport related to the gravel fraction may differ from the volume of bedload transport related to the sand fraction. Therefore the Wilcock & Crowe model (Wilcock & Crowe, 2003) makes distinction between the sediment transport related to both fractions.

First define the total amount of bedload transport q_i of fraction i (either *g* for gravel or *s* for sand) as a function of F_i (fraction size of fraction i), u_* (shear velocity of the flow), R (the submerged specific gravity of the sediment), g (gravitational acceleration) and the dimensionless bedload transport parameter W_i^* (Parker, 2004):

$$q_i = F_i \frac{u_*^3}{Rg} W_i^* \qquad (8)$$

The shear velocity of the flow is the square root of the bed shear stress divided by the water density:

$$u_* = \sqrt{\frac{\tau_{bs}}{\rho}} \qquad (9)$$

The bed shear stress is defined as a function of the average flow velocity, mass density of water and the friction coefficient due to skin friction:

$$\tau_{bs} = C_{fs} \rho u_w^2 \qquad (10)$$

Please note that only the friction coefficient due to skin friction C_{fs} (see Appendix B.4), is relevant to the calculation of the sediment process (the friction coefficient due to form drag is not applicable).

Willcock and Crowe (Wilcock & Crowe, 2003) composed a set of empirical equations in order to calculate the dimensionless bedload transport parameter W_i^*:

$$W_i^* = \begin{cases} 0.002\varphi^{7.5} & \text{for } \varphi < 1.35 \\ 14\left(1-\dfrac{0.894}{\varphi^{0.5}}\right)^{4.5} & \text{for } \varphi \geq 1.35 \end{cases} \tag{11}$$

$$\varphi_i = \frac{\tau_{sg}^*}{\tau_{ssrg}^*}\left(\frac{D_x}{D_{sg}}\right)^{-b} \tag{12}$$

$$\tau_{ssrg}^* = 0.021 + 0.015\exp(-20F_s) \tag{13}$$

$$\tau_{sg}^* = \frac{u_*^2}{RgD_{sg}} \tag{14}$$

$$b = \frac{0.67}{1+\exp(1.5 - D_x / D_{sg})} \tag{15}$$

In these equations is D_i the characteristic sediment size of fraction *i*, are *b* and φ both dimensionless parameters, is F_s the volume fraction of sand, τ_{sg}^* the dimensionless Shields number related to the surface geometric mean size of sediment, τ_{ssrg}^* the reference dimensionless Shields stress for mean size of bed surface and is u_* the shear velocity of the flow as defined in Equation (9). The parameter D_{sg} is defined as the surface geometric mean size which is a function of the fraction sizes and the grain sizes corresponding to these fractions:

$$D_{sg} = 2^{\phi_{sg}} \tag{16}$$

$$\phi_{sg} = \phi_g F_{mg} + \phi_s F_{ms} \tag{17}$$

$$\phi_i = {}^2\log(D_i) \tag{18}$$

It is now possible to calculate both the bedload sand and gravel transport using Equation (8). The total bedload transport sediment is the sum of the bedload transport corresponding to both fractions:

$$q = q_s + q_g \tag{19}$$

2.2.2 Propagation velocity of the bedload sediment

For the calculation of the propagation velocity of the bedload sediment, diverse (dimensionless) parameters have to be calculated as input for the empirical model. The following derivation is the most suitable according to Jelle van der Zwaag (based on: van Rijn, 1993).

The analysis yields for both fractions where the subscript *i* stands for either gravel (g) or sand (s).

$$u_i = u_{cr;i}^*\left(10 - 7\left(\frac{\tau_{cr;i}^*}{\tau^*}\right)^{0.5}\right) \tag{20}$$

$$u_{cr;i}^* = \sqrt{\frac{\tau_{cr;i}}{\rho}} \tag{21}$$

$$\tau_{cr;i} = \tau^*_{cr;i}\left(\rho_s - \rho\right) g D_i \tag{22}$$

$$\tau^*_{cr;i} = 0.013\left(D^*_i\right)^{0.29} \tag{23}$$

$$D^*_i = \left(\frac{Rg}{\nu^2}\right)^{1/3} D_i \tag{24}$$

In this derivation ν is the kinematic viscosity, D^* a dimensionless sediment size, D the characteristic sediment size, R the submerged specific gravity of the sediment, *g* the gravitational acceleration, τ^*_{cr} a dimensionless critical shear stress, τ_{cr} the critical shear stress, u^*_{cr} the critical shear stress velocity of the sediment and u the average propagation velocity of the bedload sediment.

The dimensionless shear stress in Equation (20) is the same for both fractions and is defined as:

$$\tau^* = \frac{\tau_{bs}}{Rg\mathrm{D}_{s50}} \tag{25}$$

In which the dimensionless bed shear stress τ_{bs} is defined by Equation (10) and D_{s50} is the bed surface sediment size of the 50% percentile which we approximate with the surface geometric mean size defined in Equation (16) (reason for this approximation is that the median size of the sediment mixture is very clumsy in a two fractional schematisation).

2.2.3 Upstream flow depth

The upstream flow depth can be calculated with the equation of Belangér as derived in Appendix B.3.

$$\frac{dH}{dx} = \frac{S - S_f}{1 - Fr^2} \tag{26}$$

In which *H* the flow depth, S_f the friction slope and *Fr* the Froude number. For the bedslope *S* yields:

$$S = -\frac{\partial \eta}{\partial x} \tag{27}$$

The Froude number is a function of the water discharge, the gravitational acceleration and the flow depth (Parker, 2004):

$$Fr = \sqrt{\frac{q_w{}^2}{gH^3}} \tag{28}$$

For the friction slope S_f yields the following emperical system of equations (derived in Appendix B.4):

$$S_f = \left(\alpha_r \left(\frac{H_s}{k_s}\right)^{1/6} \frac{H}{q_w}\right)^{-2} \frac{1}{gH_s} \tag{29}$$

$$H_s = \left(0.05 + 0.7\left(\frac{HS_f}{RD_{s50}}\mathbf{Fr}^{0.7}\right)^{0.8}\right)\frac{RD_{s50}}{S_f} \tag{30}$$

H_s is the flow depth related to skin friction (the Einstein decomposition divides the total flow depth in two components: one related to skin friction and the other related to from drag; Appendix B.4), D_{s50} is the bed surface sediment size of the 50% percentile, α_r a dimensionless constant used in the Manning-Strickler formulation, R the submerged specific gravity of the sediment, and k_s is the roughness height.

3 Numerical schematisation

3.1 General numerical schematisation

Because most properties of the morphodynamic model vary both in time as in space, it is necessary to define a numerical grid. The symbol *i* is chosen as representing the steps in time with a total of *N* steps over a time *T*. The symbol *j* is selected for the steps in space with a total of *K* over a length of *L*. This is summarized in Figure 3. For the composition of the layers below the bed surface elevation is chosen for a third axis, perpendicular to the other two axis.

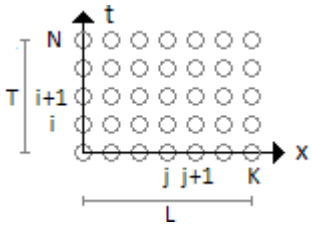

Figure 3 - Numerical grid

From now on, define the positive x direction in downstream direction and x as zero in the most upstream point of the observed river section. The initial bed surface elevation of the riverbed is defined as zero in the most downstream point. These conventions are presented in Figure 4.

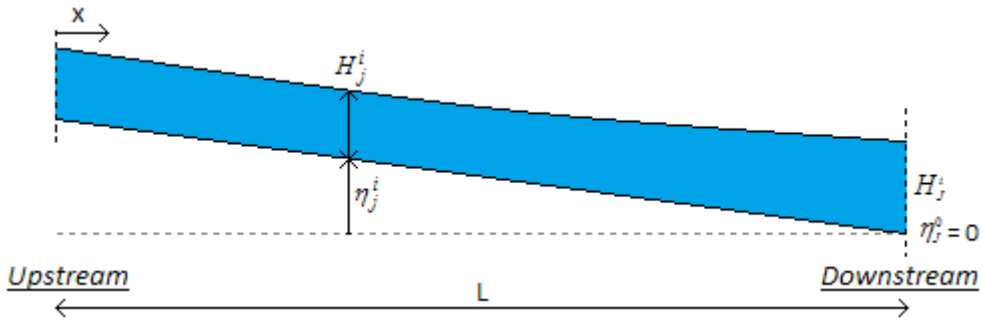

Figure 4 - Definition of the reference axis

Basis of the numerical schematisation is an explicit numerical scheme. The advantage is an uncomplicated and fast calculation method. The only drawback is that the scheme is conditionally stable (there is no complete free choice of the step size in time and space; Vuik, 2007).

Typical for the numerical stability is the Courant-Friedrichs-Levy condition which states that the time steps have to be small enough in order to let the information flow over the space gridpoints and is formulated as a function of the celerity *c* of the sediment (Schär, 2012):

$$Cr = c\frac{\Delta t}{\Delta x} \leq 1 \tag{31}$$

In order to obtain a numerical accuracy that is as high as possible, central difference is preferable over backward and forward difference (Appendix C contains a summary of the numerical schematisations with their numerical accuracies). However, explicit central difference in time is impossible due to the fact that the properties of the future are unknown. This is only possible if an implicit scheme is used, but that makes things too complicated. Therefore a backward difference in time, central difference in space BTCS schematisation is mainly used (Higham, D.J., 2004). Only in situations when central difference in space is impossible or clumsy, for example with the backwater calculations of Section 2.2.3, we make use of the backward or forward difference in space.

3.2 Numerical approximation of the equations related to morphodynamics

3.2.1 Morphological change

In order to calculate the morphological change (the bed surface elevation of the next time step), the overall equation of conservation of sediment mass, Equation (2), can be approximated with a BTCS scheme. Central difference over place at the boundaries is replaced with forward and backward difference over place. The scheme starts at *i* = 2 because backward difference over time at i = 1 is not possible:

for: i=2..N j=1

$$\eta_1^i = \eta_1^{i-1} - \frac{\Delta t}{c_b}\left(\frac{a_1^i - a_1^{i-1}}{\Delta t} + \frac{q_2^i - q_1^i}{\Delta x}\right) \tag{32}$$

for: i=2..N j=2..K-1

$$\eta_j^i = \eta_j^{i-1} - \frac{\Delta t}{c_b}\left(\frac{a_j^i - a_j^{i-1}}{\Delta t} + \frac{q_{j+1}^i - q_{j-1}^i}{2\Delta x}\right) \tag{33}$$

for: i=2...N j=K

$$\eta_K^i = \eta_K^{i-1} - \frac{\Delta t}{c_b}\left(\frac{a_K^i - a_K^{i-1}}{\Delta t} + \frac{q_K^i - q_{K-1}^i}{\Delta x}\right) \tag{34}$$

3.2.2 Volume fractions

We now apply the BTCS numerical scheme to Equation (5), the balance equation for the gravel fraction of a sand-gravel sediment mixture, and write F_{mg} at the current time step to the left hand side (F_{mg} occurs twice in the numerical schematisation of Equation (5)). We then replace central difference by forward and backward difference at the boundaries:

for: i=2..N j=1

$$F_{mg;1}^i = \frac{F_{mg;1}^{i-1} + \frac{\Delta t}{c_b \delta_1^i}\left(\begin{array}{l} -\frac{q_{g;2}^i - q_{g;1}^i}{\Delta x} - \frac{a_{g;1}^i - a_{g;1}^{i-1}}{\Delta t} + c_b F_{Ig;1}^i \frac{\delta_1^i - \delta_1^{i-1}}{\Delta t} \\ +F_{Ig;1}^i\left(\frac{q_2^i - q_1^i}{\Delta x} + \frac{a_1^i - a_1^{i-1}}{\Delta t}\right)\end{array}\right)}{\left(2 - \frac{\delta_1^{i-1}}{\delta_1^i}\right)} \tag{35}$$

for: i=2..N j=2..K-1

$$F_{mg;j}^i = \frac{F_{mg;j}^{i-1} + \frac{\Delta t}{c_b \delta_j^i}\left(\begin{array}{l} -\frac{q_{g;j+1}^i - q_{g;j-1}^i}{2\Delta x} - \frac{a_{g;j}^i - a_{g;j}^{i-1}}{\Delta t} + c_b F_{Ig;j}^i \frac{\delta_j^i - \delta_j^{i-1}}{\Delta t} \\ +F_{Ig;j}^i\left(\frac{q_{j+1}^i - q_{j-1}^i}{2\Delta x} + \frac{a_j^i - a_j^{i-1}}{\Delta t}\right)\end{array}\right)}{\left(2 - \frac{\delta_j^{i-1}}{\delta_j^i}\right)} \tag{36}$$

for: i=2..N j=K

$$F_{mg;j}^i = \frac{F_{mg;j}^{i-1} + \frac{\Delta t}{c_b \delta_j^i}\left(\begin{array}{l} -\frac{q_{g;j+1}^i - q_{g;j-1}^i}{\Delta x} - \frac{a_{g;j}^i - a_{g;j}^{i-1}}{\Delta t} + c_b F_{Ig;j}^i \frac{\delta_j^i - \delta_j^{i-1}}{\Delta t} \\ +F_{Ig;j}^i\left(\frac{q_{j+1}^i - q_{j-1}^i}{\Delta x} + \frac{a_j^i - a_j^{i-1}}{\Delta t}\right)\end{array}\right)}{\left(2 - \frac{\delta_j^{i-1}}{\delta_j^i}\right)} \tag{37}$$

3.2.3 *Upstream flow depth*

The bed slope *S* is defined as minus the spatial derivative of the bed surface elevation and can be calculated with a central in space difference. At the boundaries is it inescapable to use a differential method with less numerical accuracy:

for: j=1

$$S_1^i = -\frac{\eta_1^i - \eta_0^i}{\Delta x} \tag{38}$$

for: j=2..K-1

$$S_j^i = -\frac{\eta_{j+1}^i - \eta_{j-1}^i}{2\Delta x} \tag{39}$$

for: j=K

$$S_K^i = -\frac{\eta_K^i - \eta_{K-1}^i}{\Delta x} \tag{40}$$

A numerical backward in time predictor-corrector scheme of Equation (26) is required (Parker, 2004) to calculate the flow depth with an as high numerical accuracy as possible (subcritical flow is assumed, requiring a calculation in upstream direction):

$$H_{j-1}^i = H_j^i - \frac{1}{2}\Delta x \left[\frac{S_{j-1}^{i-1} - \left(\tilde{S}_{f1}\right)_{j-1}^i}{1 - \left(\widetilde{\mathrm{Fr}}_{j-1}^i\right)^2} + \frac{S_j^{i-1} - \left(S_{f1}\right)_j^i}{1 - \left(\mathrm{Fr}_j^i\right)^2} \right] \tag{41}$$

In which the $\tilde{S}_{f1}$ and $\widetilde{\mathrm{Fr}}$ are the predictor terms calculated with the known flow depth H_j^i. The bed slope S requires no prediction when the bed slope of the previous time step is used in the calculation (this approximation is required, otherwise would the complete time-intensive morphodynamic calculation be needed as an predictor for S).

4 Method of modelling

It is meaningful to divide the whole calculation into separate parts. The division applied in this thesis for the morphodynamic sand-gravel model is provided in Figure 5. The following paragraphs discuss each of the different calculation steps. Please note that these calculation steps are not independent of each other and that the calculation has to follow the stated sequence.

The required equations are provided in Chapter 2 and the necessary numerical schematisations are treat in Chapter 3.

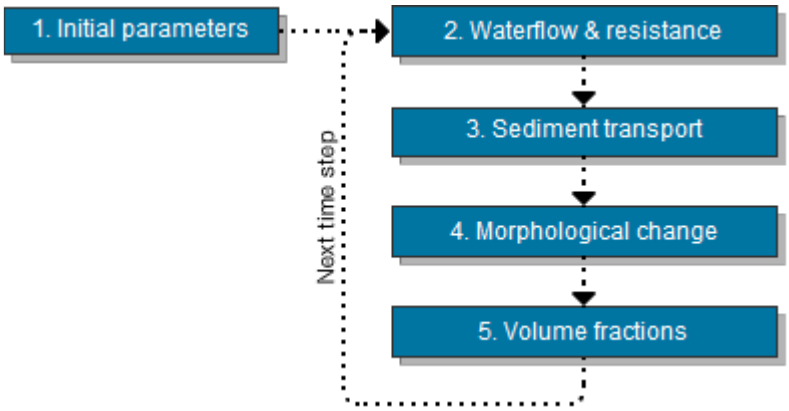

Figure 5 - Approach sand-gravel sediment model

4.1 Initial parameters

The initial parameters have a major influence on the output of the model. Therefore, it is important to make a well-founded consideration about the parameters. There are of course much more input parameters to be discussed than handled in this chapter. The aim of the following list is to handle just those parameters which might influence the method of modelling.

The sediment distribution:
The sediment of the sand-gravel morphodynamic model is schematised as two different fractions. In reality, the sediment distribution can contain a much larger variety in the sediment distribution. Therefore, a schematisation of the sediment distribution into two representative grain size fractions is required. A possible schematisation is to use the weighted average grain size with respect to the fractions in order to gain two different fractions representative for the whole mixture. Because there are only two fractions in our schematised sediment mixture, we use the grain size of the gravel fraction (the largest grain size of both fractions) as the sediment size of the 90% percentile.

Flow depth:
It would obviously be the best if the flow depth is known over the whole handled river section. However, the flow depth is known at one point in the reach during the flood event. It is possible to calculate the upstream flow depth (in the case of subcritical water flow) with the equation of Belangér, this is explained in Section 2.2.3.
Furthermore, the downstream flow depth is not known on every moment in time. The intermediate points in time can be calculated with interpolation of the data. Cubic spline interpolation is preferable over linear interpolation by the more fluent and therefore realistic functions it generates (Vuik, 2007).

Discharge:
The discharge is known at just one fixed point in space. Overall, there are two reasonable solutions:

- First, it is possible to assume that the discharge is the same over the whole handled river section and only changes in time (this quasi-stationary assumption is also made in the derivation of the equation of Belangér; see Appendix B.3).
- Second, it is possible to assume that the discharge of the river moves downstream with the velocity of the wave.

Preference is now drawn to the first option: it is the most simple method and it is based on a reasonable quasi-stationary assumption.

4.2 The actual calculation

In the previous chapters, all the required equations and schematisations are treated. The purpose of this chapter is to point out the actual calculation method. When all the required input parameters are set, it is possible to perform the calculation for the first time step. Guidance for this calculation is Figure 5.

4.2.1 Water flow & resistance

In order to calculate the flow depth at an upstream position of a point where the flow depth is known, an iterative calculation is required. The approach of the iterative process is to assume values for the flow depth H_{j-1}^{i} and the flow depth related to skin friction $\left(H_s\right)_{j-1}^{i}$ and loop through Equations (29), (30) and (41) while the difference between the value of the flow depth at a certain iteration step compared to the value of that parameter at the previous iteration step is larger than some defined accuracy.

4.2.2 Sediment transport

The sediment transport calculations are based on direct empirical equations, there is no iteration required. At this stage is it possible to calculate the specific sediment discharge and the propagation velocity of the bedload sediment for the whole river reach.

The equations which makes it possible to calculate the specific sediment discharge (the set of equations of Willcock & Crowe; 2003) are provided in Chapter 2.2.1. The propagation velocity of the bedload sediment can be calculated with the set of equations of Van Rijn (1993), see Chapter 2.2.2.

The thickness of the bedload layer can now be calculated with Equation (3).

4.2.3 Morphological change

The calculation of the morphological change is based on the overall equation of conservation of sediment. In Section 3.2.1 is this conservation equation rewritten in a numerical form.

4.2.4 Volume fractions

The gravel fractions in the active layer can be calculated with the balance equation for the gravel fraction of a sand-gravel sediment mixture. Section 3.2.2 shows the numerical schematisation of this balance equation.

The calculation for the first time step is now completed. For the next time steps (till the end of the high water surge) the same calculation as discussed above is performed. In fact, the calculation is a loop through Sections 4.2.1 up to and including Section 4.2.4.

5 Calculations on a high water wave in the Rhine

5.1 Description of the situation

In the previous chapters, the morphodynamic model is derived. This chapter uses the model to calculate the morphodynamic processes of the river section of the Rhine between Emmerich am Rhein and Lobith (Figure 6 shows the location of this river section which has a length of 10km).

Figure 6 - Location considered river section (red: upstream, green: downstream), source: maps.google.com

We consider the morphodynamic changes as a result of the flood event which took place between the 21st of January and the 15th of February in 1995. In order to calculate the flow depth with the backwater equation, the flow depth at the downstream point has to be known. The water discharge is (by the assumption of a quasi-stationary flow) constant over the river length, for example equal to the discharge at the downstream point. In conclusion, at Lobith (our downstream point) the flow depth and the water discharge are required. The data obtained from WaterBase (Dutch Ministry of Infrastructure and the Enviroment) is displayed in Figure 7. The discharge is only measured once a day and is therefore interpolated with a spline interpolation (Vuik, 2007) for continuous data availability.

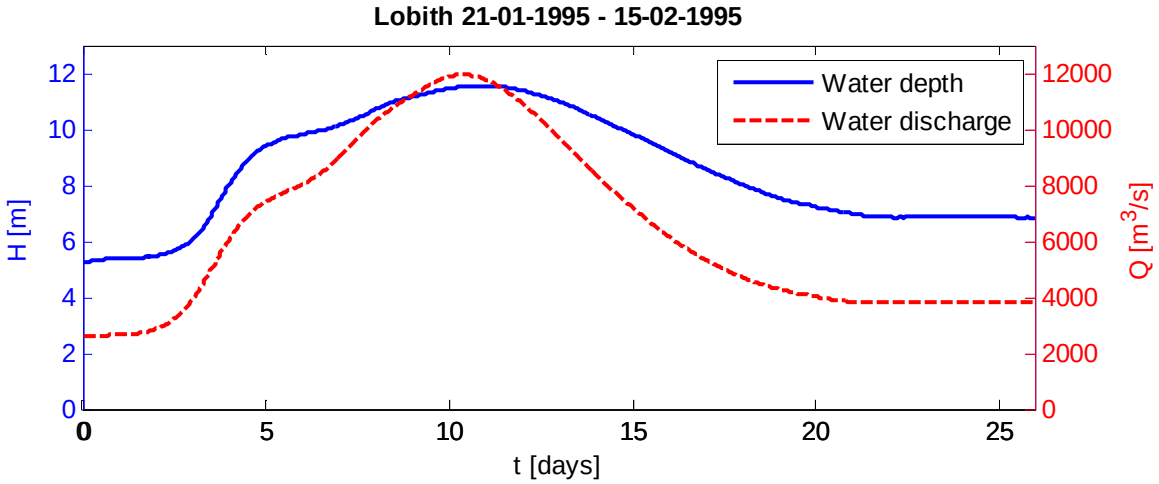

Figure 7 - Flow depth (measured hourly) and discharge (measured daily) in Lobith

As mentioned in the introduction, Jelle van der Zwaag made an overview of the input parameters relevant to the river section between Emmerich am Rhein and Lobith. The parameters that are necessary for the morphodynamic calculations are presented in Table 1.

Parameter	Value
Location riverbed Lobith	$5.1\,\text{m}$ +NAP
S : bed slope	$1.18 \cdot 10^{-4}$
c_b : sediment concentration within the bed	0.7
B : width of the river	$400\,\text{m}$
ρ_s : mass density of sediment	$2650\,\text{kgm}^{-3}$
ρ : mass density of water	$1000\,\text{kgm}^{-3}$
ν : viscosity of water	$10^{-6}\,\text{m}^2\text{s}^{-1}$
α_r : Coefficient in the Manning-Strickler equation	8.31
n_k : Coefficient in the Manning-Strickler equation	3
Sand-Gravel mixture:	
D_s	$0.0009\,\text{m}$
D_g	$0.0021\,\text{m}$
F_{0g}	0.75
$F_{mg;0}$	0.40

Table 1 - River characteristics by Jelle van der Zwaag

5.2 Results of the calculations

Based on the morphodynamic equations with its numerical schematisations, a model system in Matlab has been developed which performs the morphodynamic calculations for a sand-gravel river reach. The Matlabcode is included in Appendix D.

The sequence in which the results are presented in this chapter is based on the division made in Chapter 4 (see Figure 5 on page 10). Furthermore, the influence of the derivative of the bedload layer thickness over time on the morphodynamic changes will be handled. Please mention that although the results are treated separately in this chapter, they are all influenced by each other.

In principle, all graphs both contain data on the beginning and data on the end of the flood event. In addition, the results are also presented on the 6th, the 12th and the 18th day of the flood event (the numbers of days are on the same scale as used in Figure 7).

Figures 8-14 are generated without taking into account the time derivative of the effective thickness of the bedload transport layer. Section 5.2.5 will focus on the effect of the bedload layer on the results.

5.2.1 Flow depth

The flow depth at Lobith (the most downstream point in the observed river section, in the model located at x = 10 km) is obtained via the database of WaterBase and is displayed in Figure 7 of Section 5.1. The results of the calculations of the flow depths upstream of Lobith with the backwater equation of Section 2.2.3 are presented in Figure 8.

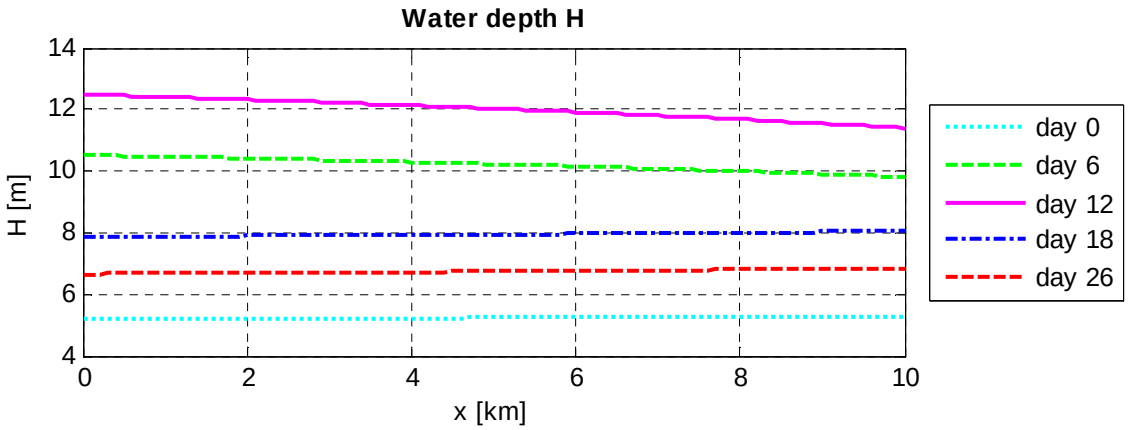

Figure 8 - Flow depth at various times

The biggest difference between the lines in Figure 8 is the vertical location (at x = 10 km is this consistent with Figure 7). However, when you look into more detail, you can see that the type of backwater curve is not for all the days the same. The flow depth curves of day 6 and day 18 are displayed in Figure 9.

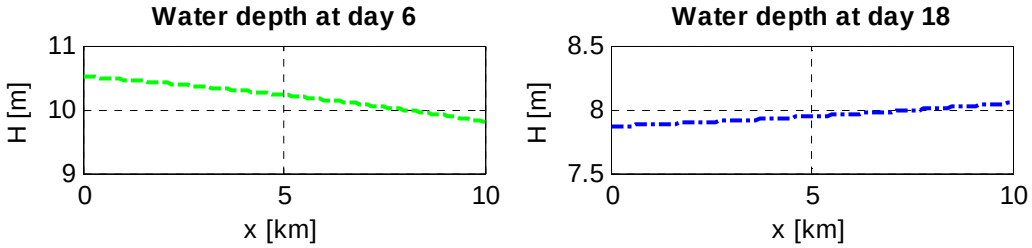

Figure 9 - Detailed flow depth variation for day 6 (M2 curve) and day 18 (M1 curve)

The flow depth curve of day 6 is a so-called M2-type curve (Battjes, 2002) which means that the Froude number is smaller than one (subcritical flow) but that the friction slope S_f is steeper than the bed slope S (see equation of Belangér, Equation (26)). On the other hand, the friction slope S_f on day 18 is less steep than the bed slope S. The Froude number on day 18 is smaller than one what results in an M1-type curve.

The variation in the shape of the curves is therefore the result of the change of sign of the bed slope S minus the friction slope S_f during the morphological processes. A physical explaination is that the downstream imposed flow depth is smaller at day 6, and larger at day 18, than the flow depth over the reach.

5.2.2 Sediment transport

The bedload transport is determined with the empirical set of equations of Wilcock and Crowe (Section 2.2.1). The left plot of Figure 8 shows the bedload transport terms corresponding to both fractions at day 6. The sum of both the bedload transport related to the gravel fraction and the sand fraction equals the total bedload transport. The total bedload discharge per unit width and time, q, is displayed in the right plot of Figure 8 for the different days.

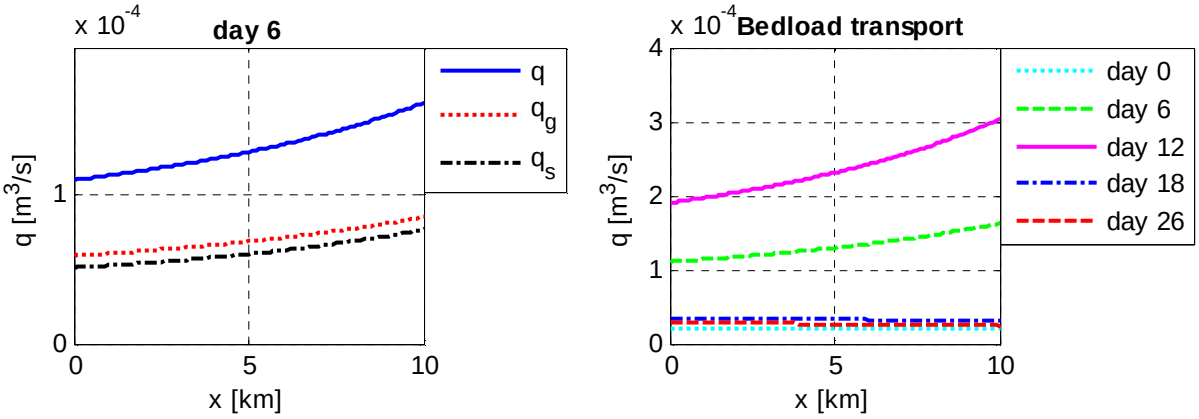

Figure 10 - Left: division corresponding to the separate fractions on day 6. Right: total bedload transport.

The increase in bedload transport in downstream direction on day 6 and day 12 can partly be explained by the fact that the flow depth at these days decreases in downstream direction. Because the discharge is constant over space at a certain moment in time (quasi-stationary assumption), the average flow velocity increases in downstream direction, which results in an increase in sediment transported in downstream direction.

As mentioned in Section 5.2.1, the flow depth curve at day 18 is of type M1 which results in an decrease of the flow velocity in downstream direction and therefore causes a decrease of the sediment transported in downstream direction. Figure 10 shows indeed a decrease of the sediment transported for day 18 in downwards direction.

5.2.3 Morphological change

The morphological change of the river bed is described by the change of the bed surface elevation. Figure 11 shows the bed surface elevation relative to the initial bed surface elevation. This figure shows an overall change of the bed surface elevation of about 1 to 2.5 cm.

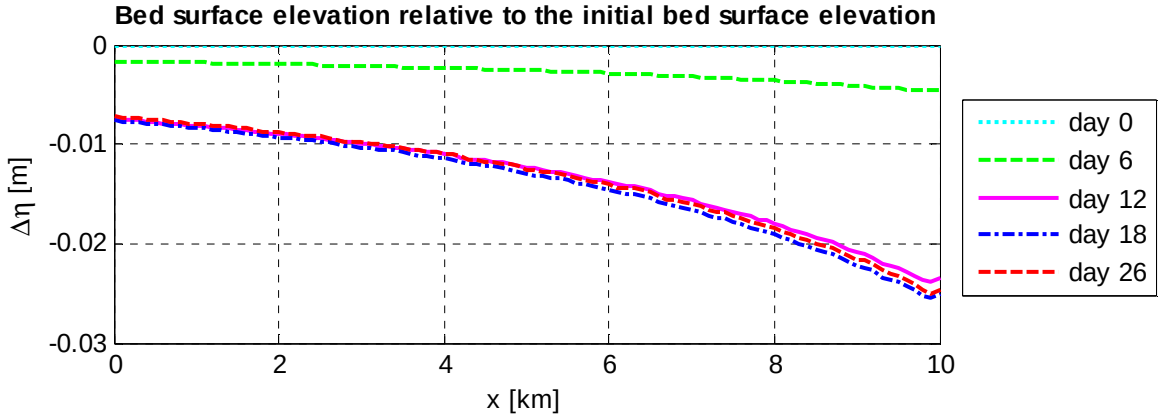

Figure 11 - Bed surface elevation relative to the initial bed surface elevation

There are two observations that stand out: the fact that there is degradation and the fact that this degradation increases in downstream direction. Both properties can be explained with the overall mass conservation equation as derived in Appendix B.1:

$$c_b \frac{\partial \eta}{\partial t} + \frac{\partial a}{\partial t} = -\frac{\partial q}{\partial x} \tag{42}$$

The change of the bed surface elevation is dominated by the spatial derivative of the bedload transport. This derivative is positive for the most part of the flood event which leads to degradation. Because this derivative is even increasing in downstream direction, the degradation is larger in the downstream part of the river section.

5.2.4 Volume fractions

Initially, the gravel fraction in the active layer is set to 40% and in the substrate equal to 75%. Both input parameters vary both in time and space due to the morphodynamic processes. The variation of the gravel fraction in the active layer is displayed in Figure 12. The increase of the gravel fraction in the active layer during the flood event can be explained as follows: mainly due to the increase in thickness of the active layer, which we defined as one fourth of the flow depth, the substrate (with a higher gravel fraction with respect to the active layer) mixes with the sediment in the active layer.

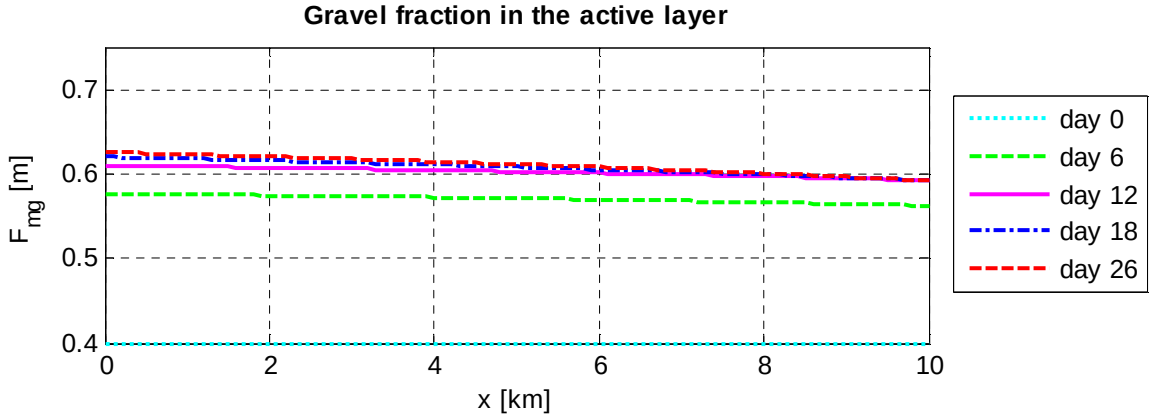

Figure 12 - Gravel fractions in the active layer

Figure 14 contains the gravel fractions below the river bed for day 12 and the final river bed (day 26). For the sake of clarity is the initial situation presented in Figure 13. Please note that the thickness of the active layer is increasing during the flood event and is decreasing for the same reason when the flow depth decreases. This process results in absorption of some of the substrate material by the active layer material during the increment of the flow depth and absorption of the active layer by the substrate during the decrement of the flow depth.

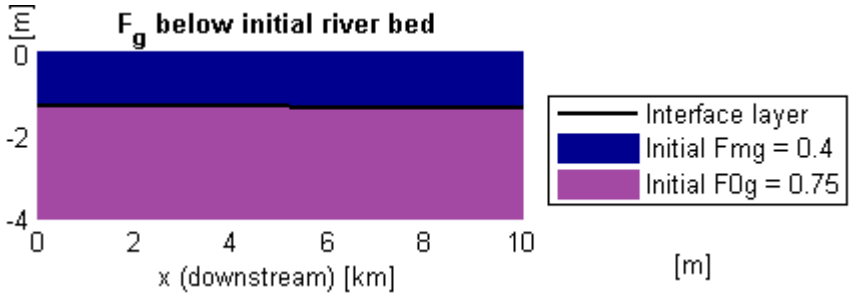

Figure 13 - Initial gravel fractions (day 0)

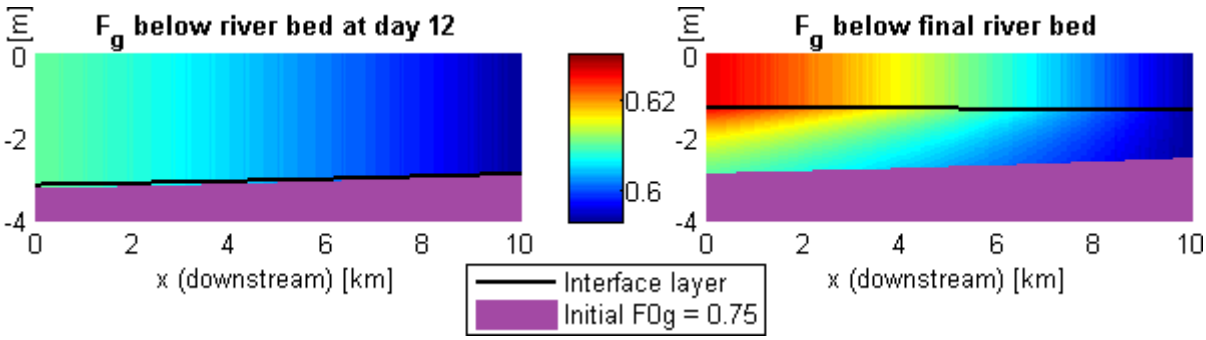

Figure 14 - Gravel fraction at day 12 (left) and day 26 (right)

5.2.5 Influence derivative of the thickness of the bedload layer over time

There are different ways to express the influence of the effective bedload transport layer over time. Because the morphodynamic processes consist of a coherent system of equations, the effective bedload layer over time can influence every process in the system. The subject we are interested in is its influence on the change in the bed surface elevation.

In order to quantify this effect, Equation (43) is used, in which the subscript *without* refers to neglecting the time derivative of the bedload layer thickness and *with* refers to taking this term into account. The subscript *initial* refers to the initial bed surface elevation.

$$\Gamma = \left| \frac{\eta_{with} - \eta_{without}}{\eta_{without} - \eta_{initial}} \right| \tag{43}$$

In summary, this number quantifies the difference in predicted bed surface elevation between neglecting and not neglecting the time derivative of the bedload layer thickness. Figure 15 shows that in the current setting of input parameters neglecting the derivative of the effective bedload transport layer results in a maximum difference in the bed surface elevation of less than 3.4%.

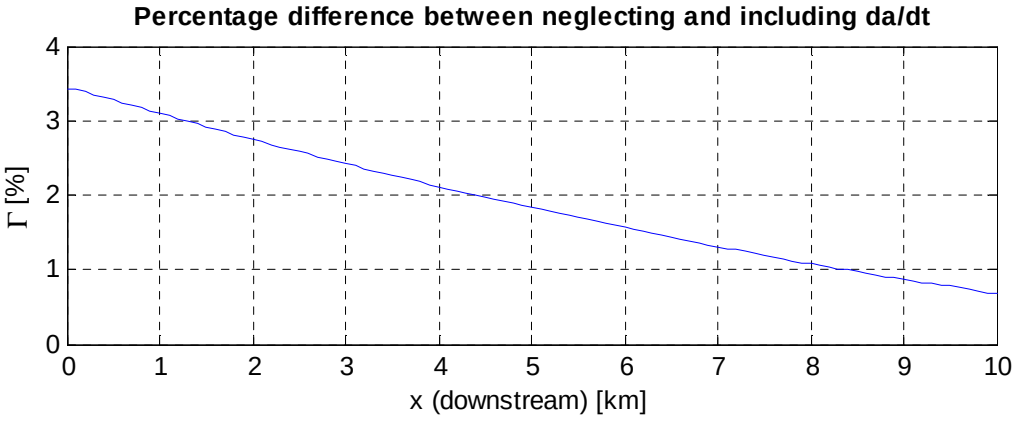

Figure 15 - The percentage difference between neglecting and not neglecting da/dt

5.2.6 *Influence derivative of the thickness of the bedload layer over time on the conservation equations*

It is interesting to investigate the influence of the derivative of the thickness of the bedload layer over time on the conservation equations. This makes it possible to conclude under what conditions the derivative over time of the bedload layer thickness is significant. In order to link the terms in the balance equations with the flood event, this chapter compares the terms with a scaled version of the flow discharge.

The first partial differential equation is the overall mass balance equation:

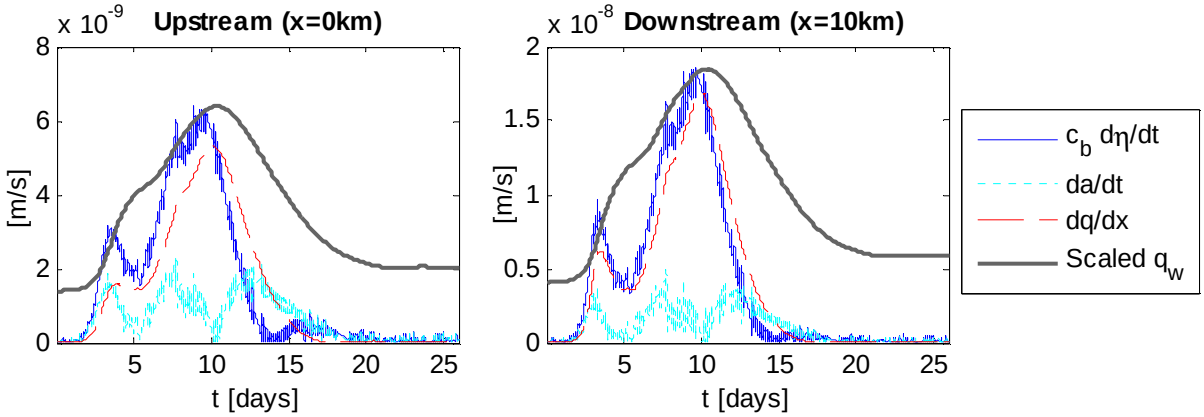

Figure 16 - Absolute size of terms in the overall balance equation.
Left: upstream position (Emmerich am Rhein). Right: downstream position (Lobith).

There are two observations that stand out of Figure 16. First, the terms at the downstream position are about twice as large, compared to the terms at the upstream position (see the different axis scales). This is in accordance with the about twice as much surface elevation at the downstream side of the river reach (see Figure 11). Second, the order of magnitude of the derivative of the bedload layer thickness over time shows peaks where the change of the flow discharge over time is maximum.

The second partial differential equation is the mass conservation equation for the sand and gravel fractions:

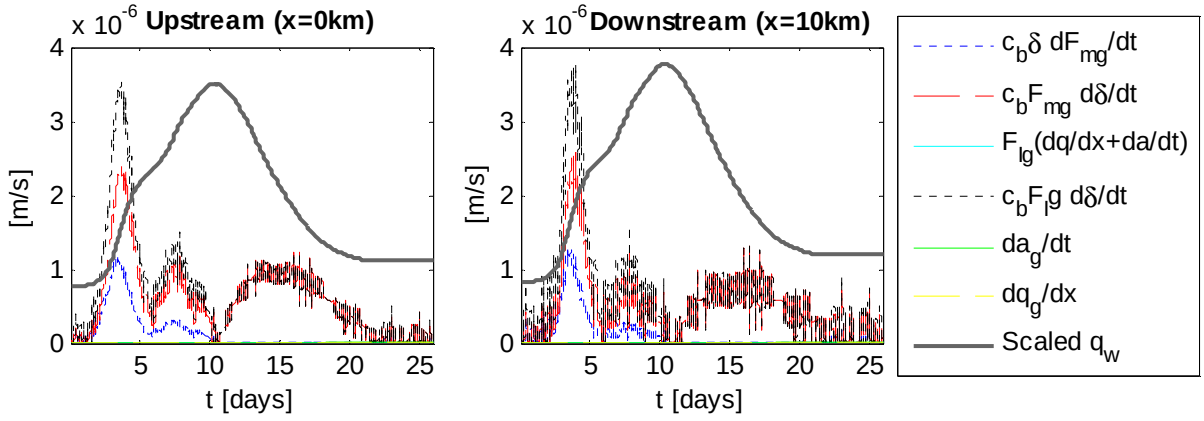

Figure 17 - Absolute Size of terms in the balance equation with distinction between both fractions.
Left: upstream position (Emmerich am Rhein). Right: downstream position (Lobith).

Figure 17 shows that all the terms which contain the derivative of the bedload layer thickness over time are not significant in the mass conservation equation for the sand and gravel fractions. However, as with the overall mass balance equation are there peaks visible in the order of magnitude of the terms where the change of the flow discharge is maximum.

6 Parameter study

This chapter aims to perform an effective parameter study in order to test the sensitivity of the result found in Section 5.2.5. The difference in predicted bed elevation between neglecting and including the time derivative of the bedload layer thickness is less than 4%, as found in the previous chapter. The question remains how big the influence of the input parameters on this result is.
It has to be clear that this parameter study is far from complete. First some parameters of interest will be selected. Subsequently these parameters are varied within a reasonable range. The point of interest is the difference in the influence of the time derivative of the thickness of the beload layer.

6.1 Parameters of interest

Due to the complexity of the set of equations, it is hard to find the most significant parameters. This chapter makes a rough selection, based on the order of the magnitude of the terms in the differential equations.

From Figure 16 and Figure 17 of Section 5.2.6, it follows that the parameters c_b, δ, F_{mg} and F_{lg} appear in terms of a significant order in the differential equation. Therefore, it seems logical to test their sensitivity. F_{lg} will be tested by varying the parameter F_{0g} and F_{mg} (which is already the point of interest). Because the sediment discharge and the thickness of the bedload layer also appear in significant terms, it might be interesting to vary the characteristic sediment sizes too.

6.2 Results of the parameter study

Varying the initial values of the parameters c_b, δ, F_{mg}, F_{0g}, D_g and D_s within a reasonable range, results in the following significances of the time derivative of the thickness of the bedload layer:

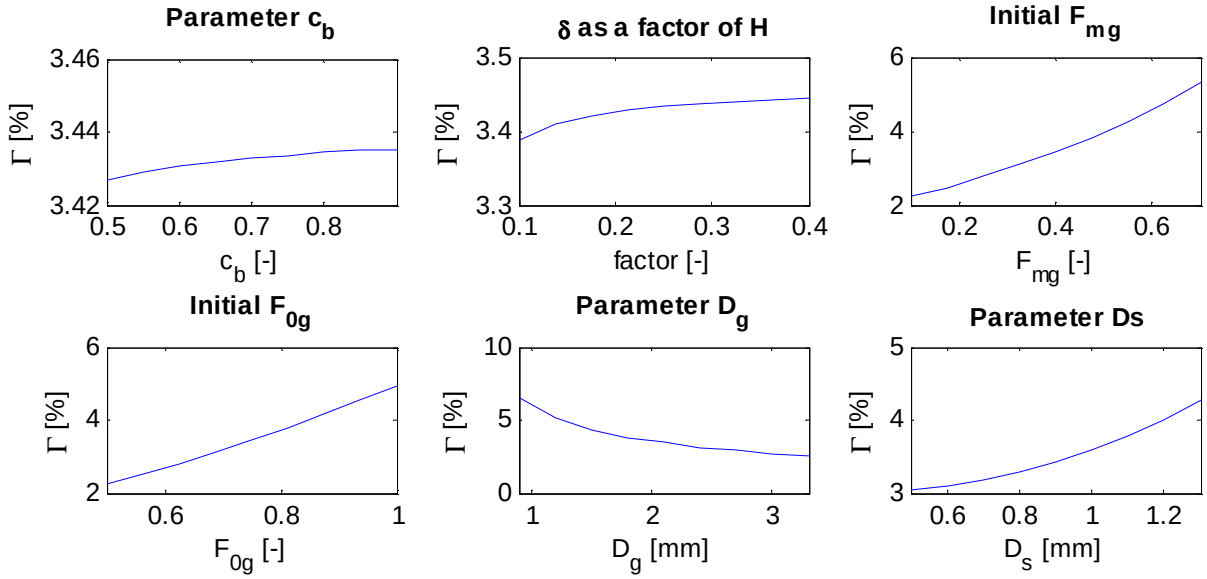

Figure 18 - Results of the parameter study

With respect to the initial parameters we find a maximum variation in the result of about a factor two with respect to the maximum of 4% influence in Section 5.2.5. The sediment parameters (F_{mg}, F_{0g}, D_g and D_s) are the most influential of the tested input parameters.
Please note that when the influence on the significance of the time derivative of the thickness of the bedload layer is small, it does not mean that the choice of input parameter is not important: they might still influence the other results in a significant way.

7 Conclusions and further research

7.1 Conclusions

With a numerical approximation of the continuity equations for sediment mass is it possible to describe the morphodynamic processes in a detailed manner. The set up of the morphodynamic model consists of many simplifications and assumptions. The main assumptions on which the model system is based are the quasi-stationary assumption, the bi-fractional schematisation of the sediment mixture, and the schematisation of the bed into layers (distinguishes the substrate, the active layer, and the bedload layer).

A calculation of the flood event between the 21st of January and the 15th of February in 1995 over the river section of the Rhine between *Emmerich am Rhein* and *Lobith* shows a less than 4% influence on the morphodynamic changes of the time derivative of the thickness of the bedload transport. Furthermore, this calculation results in an increase of the bedload transport in downstream direction, causing degradation of the river bed with a maximum of about 2 cm.

The parameter study (considering the sediment concentration of the river bed, the thickness of the active layer, the gravel fraction in the active layer and in the substrate, and the grain sizes of the sand and gravel fractions) makes clear that the time derivative is mainly influenced by the sediment properties. However, within a reasonable range of variation of those parameters, the influence of the derivative remains restricted to about a factor two with respect to the 4%.

A link is observed between the order of the magnitude of the derivative of the bedload layer thickness over time and the steepness of the derivative of the water discharge over time. It is therefore probably not necessarily a smaller or bigger flood event that would cause a larger effect with respect to the 4% influence, but a faster variation in the water discharge or a series of flood events.

Under the conditions of the Rhine between *Emmerich am Rhein* and *Lobith* it seems reasonable to assume that the thickness of the bedload layer is constant in time. However, it depends on the purpose of the calculations and the accuracy of the calculation method whether it is meaningful to or not to neglect the mentioned derivative. About 4 cm difference on a meter degradation might be acceptable for the dredging industry but it can be significant for scientific studies.

7.2 Further research

Due to the limited duration of the study (eight weeks), it is important to mention the limitations of the conclusions and propose further research to obtain a conclusion with a more scientific and practical value.

Limitations of this study:

- The sand-gravel schematisation of the sediment mixture is a discrete one. The model developed in this thesis uses, for example, the grain size of the gravel fraction as the bed surface sediment size of the 90% percentile. It is certainly meaningful to schematise the sediment mixture into more than two size fractions.
- The result of the morphodynamic changes (about 2cm degradation during a flood event) is in good agreement with the real bed elevation changes in the Rhine (about 2 cm degradation a year) assuming one flood event a year. However, the real acting 2 centimetre degradation a year might also be the cause of other acting processes like settling and shipping.
- There are processes influencing the morphodynamic changes which are not treated in the current model. One example is a shortage of sediment at the upstream boundary. A study is required to determine the exact conditions of the river section which might influence the results (one may think of river bends, varying width of the river, varying sediment transport over the width of the river and so on).
- The river section handled in this thesis (the section between Emmerich am Rhein and Lobith) is a pretty downstream located section of the Rhine with fine grain sizes. Greater grain sizes can result in different outcome of the study.
- Delta, the thickness of the active layer, is in this model proposed as one fourth of the flow depth. Section 6.2 shows that factor with respect to the flow depth does not change the outcome of this study on a significant way. However, the real acting delta might be delayed from the flow depth, causing other results.
- The initial substrate is assumed to be constant over the depth. Figure 14 shows that the composition of the substrate after the high water wave is not constant at all. A different initial substrate composition might be a good addition to the model.

Interesting further research:

- The link observed between the order of the magnitude of the derivative of the bedload layer thickness over time and the steepness of the derivative of the water discharge over time might be very interesting. It requires further research in order to determine under what conditions the derivative of the bedload layer thickness over time becomes significant.
- Whether a 4% influence is significant or not, depends on the economic and scientific conditions and the purpose of the research. It might be interesting to investigate the percentage influence for which the derivative is just significant.
- An exact determination of certain terms is senseless if other terms are completely uncertain. This research can be extended with an accuracy analysis of the other terms in the model.
- The model developed in this thesis provides more results than just the significance of the effective thickness of the bedload transport layer over time. This research did not test these results with the real acting processes in the Rhine. Such a study can increase the scientific value of the developed model.

References

Battjes, J. (2002). *Lecture notes: CT2100: Vloeistofmechanica.* TU Delft.

Blom, A. (2003). *A vertical sorting model for rivers with non-uniform sediment and dunes.* University of Twente: Ph. D. thesis.

Dutch Ministry of Infrastructure and the Enviroment. (sd). *Waterbase*. Opgehaald van Water depth and discharge data of the Rhine: http://live.waterbase.nl

Higham, D.J. (2004). *An Introduction to Financial Option Valuation.* Cambridge.

Hirano, M. (1971). River bed degradation with armouring. *Transactions Jap. Soc. Civ. Eng., 3* , 194-195.

Mathworks. (2012). *Product documentation: techniques for improving performance*. Retrieved May 1, 2012, from Matlab: http://www.mathworks.nl/help/techdoc/matlab_prog/f8-784135.html

Parker, G. (2004). *1D sediment transport morphodynamics.* University of Illinois: Powerpoint lectures e-book.

Rijn, L. v. (1993). *Principles of sediment transport in rivers, estuaries and coastal seas.* University of Utrecht.

Schär, C. (2012). *The Courant-Friedrichs-Levy (CFL) Stability Criterion.* ETH Zürich: Powerpoint lectures.

Vuik, C. (2007). *Numerical Methods for Ordinary Differential Equations.* TU Delft.

Wilcock, P., & Crowe, J. (2003). *Surface-based Transport Model for Mixed-Size Sediment.* University of Baltimore.

Wong Egoavil, M. (2006). *Model for erosion, transport and deposition of tracer stones in gravel-bed streams.* University of Minnesota: Ph. D. thesis.

Appendix A: List of symbols

a	Effective thickness of the bed transport layer	*[m]*
a_i	Effective thickness of the bed transport layer related to fraction i	*[m]*
A	Surface area	*[m^2]*
B	Width of the river	*[m]*
c	Celerity of the sediment	*[ms^{-2}]*
C	Chezy coefficient	*[$m^{1/2}s^{-1}$]*
c_b	Sediment concentration within the bed (c_b = 1 – porosity)	*[-]*
C_f	Bed resistance coefficient	*[-]*
C_{fs}	Skin friction coefficient	*[-]*
C_{ff}	Friction coefficient associated with form drag	*[-]*
Cr	Courant number	*[-]*
D	Characteristic sediment size	*[m]*
D_i	Characteristic sediment size of fraction i	*[m]*
D_{s50}	Bed surface sediment size of the 50% percentile	*[m]*
D_{s90}	Bed surface sediment size of the 90% percentile	*[m]*
D_{sg}	Surface geometric mean size of sediment	*[m]*
D^*	Dimensionless sediment size	*[-]*
$\langle E \rangle$	Relative energy head	*[m]*
F_i	Volume fraction of size fraction i	*[-]*
F_{Ii}	Volume fraction of size fraction i in the interface between the active layer and the substrate	*[-]*
F_{mi}	Volume fraction of size fraction i in the active layer	*[-]*
F_{0i}	Volume fraction of size fraction i in the substrate	*[-]*
Fr	Froude number	*[-]*
g	Gravitational acceleration	*[ms^{-2}]*
H	Flow depth	*[m]*
$\langle H \rangle$	Energy head	*[m]*
i	The time step number in the numerical model	*[-]*
j	The number of the step in space in the numerical model	*[-]*
k_s	Roughness height	*[m]*
K	Total number of steps in space in the numerical model	*[-]*
L	Length of the observed river section	*[m]*
n_k	Dimensionless number between 1.5 and 3 used in the Manning-Strickler formulation	*[-]*
N	Total number of steps in time in the numerical model	*[-]*
q	Volume of bedload transport per unit width and time (excluding pores)	*[m^2s^{-1}]*
q_i	Volume of bedload transport per unit width and time (excluding pores) related to fraction i	*[m^2s^{-1}]*

q^*	Dimensionless Einstein bedload number	*[-]*
q_w	Water discharge per unit width	*[m^2s^{-1}]*
R	Submerged specific gravity of the sediment ($R = \frac{\rho_s - \rho}{\rho}$)	*[-]*
S	Bed slope	*[-]*
S_f	Friction slope	*[-]*
t	Time	*[s]*
T	Total observed time	*[s]*
u	Average propagation velocity of sediment	*[ms^{-1}]*
u_*	Shear velocity of the flow	*[ms^{-1}]*
u_{cr}^*	Critical shear velocity of the sediment	*[ms^{-1}]*
u_w	Average flow velocity	*[ms^{-1}]*
V	Volume	*[m^3]*
W_i^*	Dimensionless transport rate of size fraction i	*[-]*
x	Position in the length axis of the river	*[m]*
α_r	Dimensionless constant between 8 and 9 used in the Manning-Strickler formulation	*[-]*
δ	Thickness of the active layer	*[m]*
Δ	Bedform height	*[m]*
Δt	Length of the time step in the numerical model	*[s]*
Δx	Length of the step in space in the numerical model	*[m]*
Γ	Dimensionless parameter used to express the influence of the time derivative of the effective bedload transport layer	*[-]*
η	Bed surface elevation	*[m]*
η_I	Elevation of the interface between the active layer and the substrate	*[m]*
ρ	Mass density of water	*[kgm^{-3}]*
ρ_s	Mass density of sediment	*[kgm^{-3}]*
τ^*	Dimensionless shear stress	*[-]*
τ_{bs}	Bed boundary shear stress	*[$kgm^{-1}s^{-2}$]*
τ_{cr}	Critical shear stress	*[$kgm^{-1}s^{-2}$]*
τ_{cr}^*	Dimensionless critical shear stress	*[-]*
τ_s^*	Dimensionless Shields number	*[-]*
τ_{sg}^*	Dimensionless Shields number related to the surface geometric mean size of sediment	*[-]*
ν	Kinematic viscosity of water	*[m^2s^{-1}]*

Appendix B: Derivations

B.1 Continuity of sediment: total sediment transport

The total bedload sediment transport, *q*, and the corresponding thickness of the bedload layer, *a*, are given by:

$$q = q_s + q_g \tag{44}$$

$$a = a_s + a_g = \frac{q_s}{u_s} + \frac{q_g}{u_g} \tag{45}$$

For the derivation of the continuity equation, we use the schematisation of Figure 19.

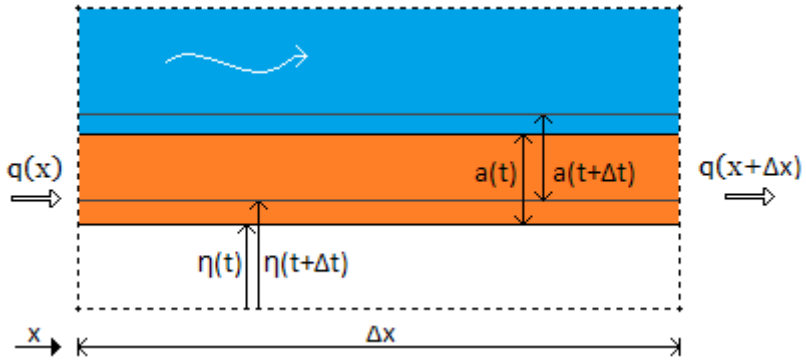

Figure 19 - Schematisation continuity area

The conservation of sediment results in the following equation (c_b is the sediment concentration; see also page 23):

$$c_b\left[\eta(t+\Delta t)-\eta(t)\right]\Delta x+\left[a(t+\Delta t)-a(t)\right]\Delta x+\left[q(x+\Delta x)-q(x)\right]\Delta t=0 \tag{46}$$

$$c_b\frac{\eta(t+\Delta t)-\eta(t)}{\Delta t}+\frac{a(t+\Delta t)-a(t)}{\Delta t}=-\frac{q(x+\Delta x)-q(x)}{\Delta x} \tag{47}$$

With a linear approximation of the Taylor expansion we find the continuity equation for the total amount of bedload transport:

$$c_b\frac{\partial\eta}{\partial t}+\frac{\partial a}{\partial t}=-\frac{\partial q}{\partial x} \tag{48}$$

As stated before, the second term in Equation (48) is almost always ignored as the term is considered to be small compared to the other terms in the equation.

B.2 Continuity of sediment: sand-gravel sediment mixture

In the case of non-uniform sediment, it is possible to derive a more detailed relationship then derived in Appendix B.1. The bedload layer thickness *a* term is divided into terms for each specific sediment fraction. This research will treat two different fractions, sand and gravel. Of course, the best would be to handle more than two fractions, but the advantage of two fractions is the following equation:

$$\sum F_i = F_1 + F_2 = 1 \tag{49}$$

When the volume fraction of one of the fractions is calculated, the volume fraction of the other fraction follows directly from this relationship. When handling more than two fractions, more equations are needed, which would increase complexity of this research.

From now on two fractions will be handled: gravel (subscript g) and sand (subscript s). Obviously, it depends on the situation which two fractions are representative, the following derivation holds for any selection of two fractions as long as they are representative for the whole mixture.

Proceeding with Equation (1), for non-uniform sediment it follows that:

$$a \equiv \frac{V}{A} = \frac{q_g \cdot \Delta t \cdot B}{u_g \cdot \Delta t \cdot B} + \frac{q_s \cdot \Delta t \cdot B}{u_s \cdot \Delta t \cdot B} = \frac{q_g}{u_g} + \frac{q_s}{u_s} \equiv a_g + a_s \tag{50}$$

Due to Equation (49), it is only necessary to apply the continuity equation for just one of the two fractions. The schematisation for the gravel fraction, according to the active plus bedload layer model, is shown in Figure 20.

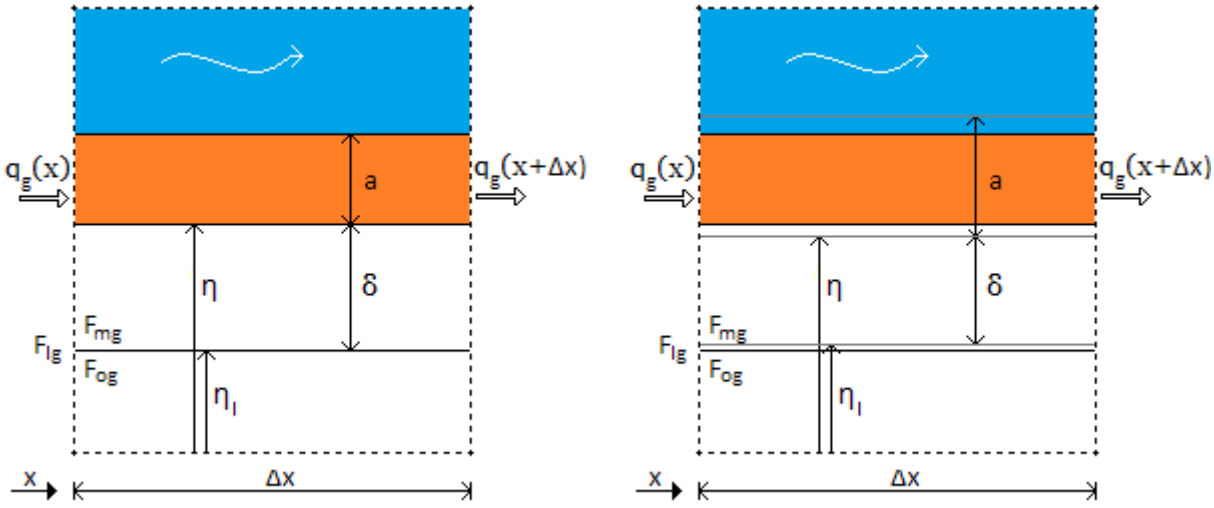

Figure 20 - Left: active plus bedload layer model, right: same model at another moment in time

The location of the interface between the active layer and the substrate is equal to the location of the bed surface minus the thickness of the active layer:

$$\eta_I = \eta - \delta \tag{51}$$

Due to conservation of the gravel fraction, the following derivation holds:

$$\begin{aligned} & c_b\left[F_{mg}(t+\Delta t)\delta(t+\Delta t)-F_{mg}(t)\delta(t)+F_{\lg}(t)\left(\eta_I(t+\Delta t)-\eta_I(t)\right)\right]\Delta x \\ & +\left[a_g(t+\Delta t)-a_g(t)\right]\Delta x+\left[q_g(x+\Delta x)-q_g(x)\right]\Delta t=0 \end{aligned} \tag{52}$$

$$\begin{aligned} & c_b\left[\frac{F_{mg}(t+\Delta t)\delta(t+\Delta t)-F_{mg}(t)\delta(t)}{\Delta t}+\frac{F_{\lg}(t)\left(\eta_I(t+\Delta t)-\eta_I(t)\right)}{\Delta t}\right] \\ & +\left[\frac{a_g(t+\Delta t)-a_g(t)}{\Delta t}\right]+\left[\frac{q_g(x+\Delta x)-q_g(x)}{\Delta x}\right]=0 \end{aligned} \tag{53}$$

A linear approximation of the Taylor expansion yields:

$$c_b\frac{\partial\left(F_{mg}\delta\right)}{\partial t}+c_bF_{\lg}\frac{\partial\eta_I}{\partial t}+\frac{\partial a_g}{\partial t}=-\frac{\partial q_g}{\partial x} \tag{54}$$

Substitution of Equation (51) gives:

$$c_b\frac{\partial\left(F_{mg}\delta\right)}{\partial t}+c_bF_{\lg}\frac{\partial(\eta-\delta)}{\partial t}+\frac{\partial a_g}{\partial t}=-\frac{\partial q_g}{\partial x} \tag{55}$$

We now substitute the overall equation of conservation of sediment, Equation (48), into Equation (55):

$$c_b\frac{\partial\left(F_{mg}\delta\right)}{\partial t}-F_{\lg}\left(\frac{\partial q}{\partial x}+\frac{\partial a}{\partial t}\right)-c_bF_{\lg}\frac{\partial\delta}{\partial t}+\frac{\partial a_g}{\partial t}=-\frac{\partial q_g}{\partial x} \tag{56}$$

Due to the product rule:

$$c_b\delta\frac{\partial F_{mg}}{\partial t}+c_bF_{mg}\frac{\partial\delta}{\partial t}-F_{\lg}\left(\frac{\partial q}{\partial x}+\frac{\partial a}{\partial t}\right)-c_bF_{\lg}\frac{\partial\delta}{\partial t}+\frac{\partial a_g}{\partial t}=-\frac{\partial q_g}{\partial x} \tag{57}$$

This is the resulting conservation equation for the gravel fraction of the sand-gravel mixture.

The volume fraction of size fraction i at the interface between the active layer and the substrate F_{Ii} depends on whether it is a case of aggradation or degradation:

$$F_{Ii}=\begin{cases} F_{mi} & \text{if} \quad \dfrac{\partial\eta_I}{\partial t}>0 \\ F_{0i} & \text{if} \quad \dfrac{\partial\eta_I}{\partial t}<0 \end{cases} \tag{58}$$

B.3. Backwater equation

The backwater equation of Belangér is used to calculate the flow depth variation. In the calculation the flow depth at the downstream location of the river (in case of subcritical flow) or the upstream location (in case of supercritical flow) is assumed to be known.

Starting point of the derivation is the formulation of energy head used by Bernoulli (Battjes, 2002):

$$\langle H \rangle = \eta + H + \frac{u_w^2}{2g} \tag{59}$$

The energy head <H> is the sum of the bed surface elevation, the water depth and the velocity head as schematised in Figure 21.

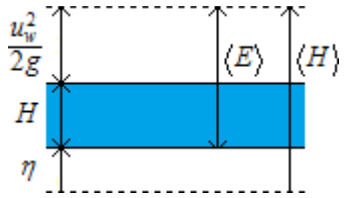

Figure 21 - Definition energy head

We can define the relative energy head <E> as:

$$\langle E \rangle = H + \frac{u_w^2}{2g} \tag{60}$$

It follows that the energy head is equal to the relative energy head plus the river bed elevation:

$$\langle H \rangle = \langle E \rangle + \eta \tag{61}$$

We define the bed slope equal to the gradient of the bed surface elevation:

$$S = -\frac{\partial \eta}{\partial x} \tag{62}$$

By definition, the friction slope is equal to the gradient of the energy head:

$$S_f = -\frac{\partial \langle H \rangle}{\partial x} \tag{63}$$

So the derivative of the relative energy head can be written as:

$$\frac{\partial \langle E \rangle}{\partial x} = \frac{\partial \langle H \rangle}{\partial x} - \frac{\partial \eta}{\partial x} = S - S_f \tag{64}$$

Under the assumption of a quasi-stationary flow, the only variable in Equation (61) is the flow depth, so the derivative of the relative energy head is equal to:

$$\frac{d\langle E \rangle}{dx} = \frac{d\langle E \rangle}{dH}\frac{dH}{dx} \tag{65}$$

Combining Equations (64) and (65) with the derivative of the relative energy head in space for which the following equation holds (Battjes, 2002):

$$\frac{d\langle E \rangle}{dH} = 1 - Fr^2 \tag{66}$$

Results in the backwater equation of Belangér:

$$\frac{dH}{dx} = \frac{S - S_f}{1 - Fr^2} \tag{67}$$

By definition (Parker, 2004):

$$Fr = \sqrt{\frac{q_w^{\ 2}}{gH^3}} \tag{68}$$

$$S_f = C_f Fr^2 = C_f \frac{q_w^{\ 2}}{gH^3} \tag{69}$$

The determination of the friction coefficient (and with that the friction slope) is treated in Appendix B.4.

In conclusion, it has to be clear that, if the flow depth variation is unknown, its calculation is an iterative process.

Please note that the direction of calculation depends on the Froude number: when the flow is subcritical (i.e. Fr < 1), the calculation has to be done in the upstream direction. Otherwise, in supercritical situations (i.e. Fr > 1), the calculation has to be done in downstream direction.

B.4. Bed resistance coefficient C_f

According to the Einstein (1950) decomposition, the bed resistance coefficient C_f contains two separate components: the skin friction coefficient C_{fs} and the friction coefficient associated with form drag C_{ff} :

$$C_f = C_{fs} + C_{ff} \tag{70}$$

Wright and Parker (2004) define the Shields number related to skin friction as a function of the overall Shields number and the Froude number with an empirical relationship:

$$\tau_s^* = 0.05 + 0.7\left(\tau^* \mathbf{Fr}^{0.7}\right)^{0.8} \tag{71}$$

This relation is designed to be used with the following formulation of the skin friction coefficient:

$$C_{fs}^{-1/2} = \frac{\alpha_r}{\alpha_{strat}}\left(\frac{H_s}{k_s}\right)^{1/6} \tag{72}$$

in which α_{strat} is a correction for flow stratification (assumed equal to 1), H_s is the mean water depth associated with skin friction. The roughness height k_s is assumed equal to three times D_{s90} .

As a result of the Einstein decomposition, we can distinguish between the flow depth associated with skin friction H_s and the flow depth associated with form drag H_f. The sum of the flow depth associated with skin friction and the flow depth associated with form drag is equal to the actual flow depth. Similarly, the following definitions applies:

$$\tau_{bs} = \rho C_{fs} u_w^2 = \rho g H_s S_f \tag{73}$$

$$\tau_{bf} = \rho C_{ff} u_w^2 = \rho g H_f S_f \tag{74}$$

$$\tau_b = \tau_{bs} + \tau_{bf} = \rho\left(C_{fs} + C_{ff}\right)u_w^2 = \rho g\left(H_s + H_f\right)S_f \tag{75}$$

Applying $u_w = q_w/H$ to Equation (73) and rewriting C_{fs} to the left-hand side:

$$C_{fs} = g H_s S_f \frac{H^2}{q_w^2} \tag{76}$$

Substitution of Equation (78) in Equation (72) with the correction for flow stratification equal to one results in:

$$\frac{q_w}{H\sqrt{g H_s S_f}} = \alpha_r\left(\frac{H_s}{k_s}\right)^{1/6} \tag{77}$$

Parker defines for the Shields number related to skin friction and the overall Shields number respectively:

$$\tau_s^* = \frac{H_s S_f}{R D_{s50}} \tag{78}$$

$$\tau^* = \frac{H S_f}{R D_{s50}} \tag{79}$$

Substitution of Equations (78) and (79) in the empirical relation of Wright and Parker (Equation (71)):

$$\frac{H_s S_f}{RD_{s50}} = 0.05 + 0.7\left(\frac{HS_f}{RD_{s50}}\mathbf{Fr}^{0.7}\right)^{0.8} \qquad (80)$$

When H is known, H_s and S_f can be computed iteratively from Equations (77) and (80).

The parameter D_{s50}, the median size of the sediment mixture, is very clumsy in a two fractional schematisation (causes numerical problems). We replace therefore this parameter by the surface geometric mean size of sediment, D_{sg}, as a approximation of the median size of the sediment mixture.

Appendix C: Numerical schemes

The numerical differential schemes presented in this appendix are derived with Taylor expansions (Vuik, 2007). For differential over time yields analogue schemes.

Forward difference in space:

$$f'(x) = \frac{f(x+\Delta x) - f(x)}{\Delta x} + \mathrm{O}(\Delta x) \tag{81}$$

Backward difference in space:

$$f'(x) = \frac{f(x) - f(x-\Delta x)}{\Delta x} + \mathrm{O}(\Delta x) \tag{82}$$

Central difference in space:

$$f'(x) = \frac{f(x+\Delta x) - f(x-\Delta x)}{2\Delta x} + \mathrm{O}\left((\Delta x)^2\right) \tag{83}$$

Please note that central difference in space has a numerical deviation of the second order whereas the other two difference methods have a deviation of the first order and are therefore less accurate.

Appendix D: Matlab model

See appendix E for the custom-made functions used in this model:

- Waterbase_load.m (page 38)

```
%% Input
% Neglecting da/dt term?
dadt = 1;           % 0 if neglecting, otherwise 1

% General parameters
g = 9.81;           % [m/s^2]

% Manning-Strickler parameters by parker
alpha_r = 8.32;     % [-]
nk = 3;             % [-]

% Sediment parameters
F_0g = 0.75;        % [-]
F_mg_0 = 0.4;       % [-] Initial gravel fraction
Dg = 0.0021;        % [m]
Ds = 0.0009;        % [m]
Ds90 = Dg;          % [m]
v = 10^-6;          % [-]

% Riverbed parameters
bedslope=1.18*10^-4;% [-] Initial bed slope
cb = 0.7;           % [-] 1-porosity
rho_s = 2650;       % [kg/m^3]
rho = 1000;         % [kg/m^3]
R = rho_s/rho-1;    % [-]

% River parameters
LOBITH_H = waterbase_load('data/H_lobith.txt'); % t=0: 21-01-1995 00:00
LOBITH_Q = waterbase_load('data/Q_lobith.txt'); % t=0: 21-01-1995 00:00
NAP_RIVERBED_LOBITH = 5.1; % [m]
B = 400;            % [m]

% Parameters for subsoil composition registration (shortened by scr)
scr_max = 3;        % [m] Maximum registration depth/height
scr_step = 0.0005;  % [m] Step size in vertical direction of the grid
scr_steps = scr_max/scr_step.*2+1; % [-] Total number of steps

%% Defining the grid
T = 2242800;        % length time interval [s]
L = 10000;          % length space interval [m]
dt = 100;           % steps in time [s]
dx = 100;           % steps in space [m]
N = T/dt+1;         % number of grid points in time [-]
K = L/dx+1;         % number of grid points in space [-]


%% Interpolation with splines of the H and Q
H_spline = interp1(LOBITH_H.T,LOBITH_H.DATA,0:dt:T,'spline')/100; % From
[cm] to [m]
Q_spline = interp1(LOBITH_Q.T,LOBITH_Q.DATA,0:dt:T,'spline');
```

```
%% Predefining the variables in the grid (x,t), (x=0: upstream)
q       = zeros(K,N);
q_g     = zeros(K,N);
q_s     = zeros(K,N);
qw      = zeros(K,N);
a       = zeros(K,N);
a_g     = zeros(K,N);
a_s     = zeros(K,N);
delta   = zeros(K,N);
H       = zeros(K,N);
Hs      = zeros(K,N);
eta     = zeros(K,N);
detaI_dt= zeros(K,N);
S       = zeros(K,1);
F_mg    = zeros(K,N);
F_Ig    = zeros(K,N);
U_shear = zeros(K,1);
Tau_dl  = zeros(K,1);
q_dl    = zeros(K,1);
soil_composition = zeros(K,scr_steps);

%% Filling in the boundary conditions and calculation for the first
timestep i=1 (t=0)
qw(:,:) = (Q_spline'*ones(1,K))'./B;
H(K,:)=H_spline'-NAP_RIVERBED_LOBITH*ones(N,1);

% River bed
eta(:,1) = bedslope*(L:-dx:0);

% S(t=0)
S(1) = -(eta(2,1)-eta(1,1))/dx;
S(2:K-1) = -(eta(3:K,1)-eta(1:K-2,1))/(2*dx);
S(K) = -(eta(K,1)-eta(K-1,1))/dx;

% Initial fractions
F_mg(:,1) = F_mg_0;
F_Ig(:,1) = F_mg(:,1);

% Calculation of ks = nk*Ds90
ks = linspace(nk*Ds90,nk*Ds90,K)';

% Calculation of initial soil composition and the location of the interface
bed layer
soil_composition(:,1:scr_max/scr_step+1) = F_0g;
soil_composition(:,scr_max/scr_step+2:scr_steps) = F_mg_0;

%% Calculation loop for the next timesteps
for i = 1:1:N % Time

    if i == 1
        phi_s = log(Dg.*1000)/log(2).*F_mg(:,1)+log(Ds.*1000)/log(2).*(1-
F_mg(:,1));
    else
        phi_s = log(Dg.*1000)/log(2).*F_mg(:,i-1)+log(Ds.*1000)/log(2).*(1-
F_mg(:,i-1));
    end
    Dsg = (2.^phi_s)./1000; % [m]
    Ds50 = Dsg;

    % Step 1: calculate the water depth
```

```
    % 1a: Calculation of Hs(K,i) via iteration
    Hs_1 = H(K,i); % First rough approximations
    o = 1;
    while o == 1 || abs(Hs_1 - Hs_1str) > 10^-4
        Hs_1str = Hs_1; % Remember the previous value
        Sf_1 = (alpha_r*(Hs_1str/ks(K)).^(1/6).*H(K,i)./qw(K,i)).^(-
2).*1/(g.*Hs_1str);
        Hs_1 =
(0.05+0.7*((H(K,i)*Sf_1/(R*Ds50(K)))*(qw(K,i)/(sqrt(g)*(H(K,i).^(3/2))))^0.
7)^0.8)*(R*Ds50(K))/(Sf_1);
        o = o + 1;
    end
    Hs(K,i) = Hs_1;

    % 1b: Calculation of H(j,i) and Hs(j,i)
    for j = K-1:-1:1
        % Calulation of the necessery parameters at j+1 (=subscript 2)
        H_2 = H(j+1,i);
        Hs_2 = Hs(j+1,i);
        Fr_2 = sqrt(qw(j+1,i)^2/(g*H_2^3));
        Sf_2 = (alpha_r*(Hs_2/ks(j)).^(1/6).*H_2./qw(j+1,i)).^(-
2).*1/(g.*Hs_2);

        % Calculation of H and Hs at j (=subscript 1)
        H_1 = H_2; Sf_1 = Sf_2; Hs_1 = Hs_2; % First approximation based on
next time step
        o = 1;
        while o == 1 || abs(H_1 - H_1str) > 10^-4
            H_1str = H_1; Hs_1str = Hs_1; % Remember the previous values
            Sf_1 = (alpha_r*(Hs_1str/ks(j)).^(1/6).*H_1str./qw(j,i)).^(-
2).*1/(g.*Hs_1str);
            Hs_1 =
(0.05+0.7*((H_1str*Sf_1/(R*Ds50(j)))*(qw(j,i)/(sqrt(g)*(H_1str.^(3/2))))^0.
7)^0.8)*(R*Ds50(j))/(Sf_1);
            Fr_1 = sqrt(qw(j,i)^2/(g*H_1str^3));
            H_1 = H_2-dx.*(1/2).*((S(j+1)-Sf_2)./(1-Fr_2.^2)+(S(j)-
Sf_1)./(1-Fr_1.^2));
            o = o + 1;
        end
        H(j,i) = H_1;
        Hs(j,i) = Hs_1;

        if Fr_1 >= 0.8
            error(['Error: Fr >=0.8, downstream calculation
required.',10,'i : ',num2str(i)])
        end
    end

    if i == 1
        % For i = 1 only determination of the delta
        % Delta(i=1)
        delta(:,1) = 0.25.*H(:,1);

        % Location of the initial interface layer
        initial_interface_location = eta(:,1)-delta(:,1); % Reference point
is the initial bedsurface location on the downstream point
    else

        % Step 2: calculate the sediment transport
        Cfs_q = (alpha_r*(Hs(:,i)./(ks)).^(1/6)).^(-2);
```

```
        Cf_q = Cfs_q; % Only associated with skin friction
        Uw = qw(:,i)./H(:,i);
        Tau_b = Cf_q.*rho.*Uw.^2;
        U_shear = sqrt(Tau_b./rho);
        tau_sg_dl = (U_shear.^2)./(R.*g.*Dsg);
        tau_ssrg_dl = 0.021+0.015.*exp(-20.*(1-F_mg(:,i-1)));
        % q_g(t=i)
        b = 0.67./(1+exp(1.5-Dg./Dsg));
        phi=tau_sg_dl./tau_ssrg_dl.*(Dg./Dsg).^(-b);
        W_dl = 0.002.*phi.^7.5.*(phi<1.35)+14.*(1-
0.894./(phi.^0.5)).^(4.5).*(phi>=1.35);
        q_g(:,i) = F_mg(:,i-1).*(U_shear.^3)./(R.*g).*W_dl;
        % q_s(t=i)
        b = 0.67./(1+exp(1.5-Ds./Dsg));
        phi=tau_sg_dl./tau_ssrg_dl.*(Ds./Dsg).^(-b);
        W_dl = 0.002.*phi.^7.5.*(phi<1.35)+14.*(1-
0.894./(phi.^0.5)).^(4.5).*(phi>=1.35);
        q_s(:,i) = (1-F_mg(:,i-1)).*(U_shear.^3)./(R.*g).*W_dl;
        % q (t=i)
        q(:,i) = q_s(:,i)+q_g(:,i);

        % U_sediment
        Tau_dl = Tau_b./(rho.*R.*g.*Ds50);
        Dg_str = (R.*g./(v.^2)).^(1/3).*Dg;
        Ds_str = (R.*g./(v.^2)).^(1/3).*Ds;
        Tau_g_cr_str = 0.013.*Dg_str.^0.29;
        Tau_s_cr_str = 0.013.*Ds_str.^0.29;
        Tau_g_cr = Tau_g_cr_str.*(rho_s-rho).*g*Dg;
        Tau_s_cr = Tau_s_cr_str.*(rho_s-rho).*g*Ds;
        Ug_str = sqrt(Tau_g_cr./rho);
        Us_str = sqrt(Tau_s_cr./rho);
        Ug = Ug_str.*(10-7.*sqrt(Tau_g_cr_str./Tau_dl));
        Us = Us_str.*(10-7.*sqrt(Tau_s_cr_str./Tau_dl));

        % a_g (t=i)
        a_g(:,i) = q_g(:,i)./Ug;
        % a_s (t=i)
        a_s(:,i) = q_g(:,i)./Us;
        % a (t=i)
        a(:,i) = a_g(:,i)+a_s(:,i);

        % Step 3: calculate  morphological change
        % Eta(t=i)
        eta(1,i) = eta(1,i-1) - dt/cb*((q(2,i)-q(1,i))/(dx)+dadt.*(a(1,i)-
a(1,i-1))/dt);
        eta(2:K-1,i) = eta(2:K-1,i-1) - dt./cb.*((q(3:K,i)-q(1:K-
2,i))./(2*dx)+dadt.*(a(2:K-1,i)-a(2:K-1,i-1))/dt);
        eta(K,i) = eta(K,i-1) - dt/cb*((q(K,i)-q(K-
1,i))/(dx)+dadt.*(a(K,i)-a(K,i-1))/dt);
        % S(t=i)
        S(1) = -(eta(2,i)-eta(1,i))/dx;
        S(2:K-1) = -(eta(3:K,i)-eta(1:K-2,i))/(2*dx);
        S(K) = -(eta(K,i)-eta(K-1,i))/dx;

        % Step 4: calculate change in volume fractions
        % Delta(t=i)
        delta(:,i) = 0.25.*H(:,i);
        % deta_I(t=i)
        detaI_dt(:,i) = (eta(:,i)-eta(:,i-1))./dt-(delta(:,i)-delta(:,i-
1))./dt;
        % F_Ig(t=i)
```

```
        current_interface_location = eta(:,i)-delta(:,i);
        relative_current_interface_location = current_interface_location -
initial_interface_location; % Relative to
        for j = 1:K

            if detaI_dt(j,i)>0
                % Increasing
                F_Ig(j,i) = F_mg(K,i-1);
            else
                % Decreasing --> use F_0g just below the interface layer
                F_Ig(j,i) =
soil_composition(j,floor((relative_current_interface_location(j)+scr_max)./
scr_step+1));
            end
        end

        % F_mg(t=i)
        if i == 2
            F_mg(:,i) = F_mg(:,i-1);
        else
            F_mg(1,i)=(F_mg(1,i-1)+dt./(cb.*delta(1,i)).*(...
                -(q_g(2,i)-q_g(1,i))./(dx)...
                +F_Ig(1,i).*((q(2,i)-q(1,i))./(dx)+dadt.*(a(1,i)-a(1,i-
1))./dt)...
                +cb.*F_Ig(1,i).*(i~=2).*(delta(1,i)-delta(1,i-1))./dt...
                -dadt.*(a_g(1,i)-a_g(1,i-1))./dt))./(2-(delta(1,i-
1))./delta(1,i));
            F_mg(2:K-1,i)=(F_mg(2:K-1,i-1)+dt./(cb.*delta(2:K-1,i)).*(...
                -(q_g(3:K,i)-q_g(1:K-2,i))./(2.*dx)...
                +F_Ig(2:K-1,i).*((q(3:K,i)-q(1:K-
2,i))./(2.*dx)+dadt.*(a(2:K-1,i)-a(2:K-1,i-1))./dt)...
                +cb.*F_Ig(2:K-1,i).*(i~=2).*(delta(2:K-1,i)-delta(2:K-1,i-
1))./dt...
                -dadt.*(a_g(2:K-1,i)-a_g(2:K-1,i-1))./dt))./(2-(delta(2:K-
1,i-1))./delta(2:K-1,i));
            F_mg(K,i)=(F_mg(K,i-1)+dt./(cb.*delta(K,i)).*(...
                -(q_g(K,i)-q_g(K-1,i))./(dx)...
                +F_Ig(K,i).*((q(K,i)-q(K-1,i))./(dx)+dadt.*(a(K,i)-a(K,i-
1))./dt)...
                +cb.*F_Ig(K,i).*(i~=2).*(delta(K,i)-delta(K,i-1))./dt...
                -dadt.*(a_g(K,i)-a_g(K,i-1))./dt))./(2-(delta(K,i-
1))./delta(K,i));
        end

        % Set above the interface layer the soil composition to the current
F_mg
        for j = 1:K

soil_composition(j,ceil((relative_current_interface_location(j)+scr_max)./s
cr_step+1):scr_steps) = F_mg(j,i);
        end
    end

end
```

Appendix E: Custom-made Matlab functions

The functions presented in this appendix are custom made and are required to run the Matlab of the previous appendices.

Waterbase_load.m

```
%% Load the waterbase data and put it in matrices
function D = waterbase_load(fname)

[a1, a2] = textread(fname, '%f  %f', 'delimiter', ';');
D.T = a1;
D.DATA = a2;
```